Front. Electr. Electron. Eng. China (2006) 2: 188–193
DOI 10.1007/s 11460-006-0022-3

RESEARCH ARTICLE

NIU Fa-liang, HUANG Jin, YANG Jia-qiang, CHEN Li-yuan, JIN Hai

Rotor broken-bar fault diagnosis of induction motor based on HHT of the startup electromagnetic torque

Abstract This paper presents a new method for rotor broken-bar fault diagnosis of induction motors. The asymmetry of the rotor caused by broken-bar fault will give rise to the appearance of additional frequency component of $2sf_s$ (s is slip and f_s is supply frequency) in the electromagnetic torque spectrum. The startup electromagnetic torque signal is decomposed into several intrinsic mode function (IMF) with empirical mode decomposition (EMD) based on the Hilbert-Huang Transform. Then, using the instantaneous frequency extraction principle of the Hilbert Transform, the rotor broken-bar fault characteristic frequency of $2sf_s$ can be exactly extracted from the IMF component, which includes the rotor fault information. Moreover, the magnitude of the IMF which includes the rotor fault information can also give the number of rotor broken bars. Experimental results demonstrate that the proposed electromagnetic torque-based fault diagnosis method is feasible.

Keywords Electromagnetic torque, Fault diagnosis, Induction motor, Hilbert-Huang transform (HHT)

1 Introduction

The rotor bar and end ring can be easily cracked due to long startup time, high load level or startup and brake frequently for induction motors. Researches show that rotor broken-bar fault accounts for almost 10 % of total induction motor failures. Consequently, early detection and evaluation of the rotor broken-bar numbers is becoming increasingly important [1]. A full fault diagnostic method should be composed of the following three steps: 1) extraction of the fault feature; 2) recognition of the fault; 3) evaluation of the fault severity or the computation of the diagnostic indexes.

The motor current signature analysis (MCSA) has been widely used due to its noninvasive property [2]. But Belling et al. [3] pointed out that while current spectrum can be used to identify rotor bar fault, predicting the severity of the fault is difficult. This has motivated researchers to investigate alternative parameters for fault diagnosis such as Park's vector modulus of the stator current, instantaneous power and electromagnetic torque, etc. [4–8]. These parameters composed of multiple input voltage and current signals of the machine offer more information than the one phase current. In fact, because the instantaneous power is comprised of the stator copper losses and the stator core losses, there will be big errors when analyzing the rotor fault severity if the motor is under low load level or with small inertias [6]. As the electromagnetic torque represents the combined effect of all the flux linkages and currents in both stator and rotor, it is highly sensitive to any asymmetrical operating condition. Theoretically, next to rotor current, the electromagnetic torque is the diagnostic medium most affected by rotor faults [7]. The electromagnetic torque related to load level and the losses is constant when the motor is healthy. But for a motor with rotor broken-bar fault, the asymmetry of the rotor will give rise to the appearance of negative component as well as positive component in the rotor rotating fields. The negative rotor field interacting with the stator field produces an additional frequency component of $2sf_s$ in the electromagnetic torque spectrum. Obviously, the frequency of the fault feature torque component is related to the slip and the supply frequency. When the motor is operating under stable conditions, the fluctuation of the supply frequency or the slip derived from such load fluctuation can produce a similar frequency component, which can be confused with the rotor fault feature component in the electromagnetic torque signal. Consequently, the rotor broken-bar fault can't be directly confirmed only through the electromagnetic

Translated from *Proceedings of the Chinese Society for Electrical Engineering*, 2005, 25(11):107-112 (in Chinese)

NIU Fa-liang(✉), HUANG Jin, YANG Jia-qiang
College of Electronic Engineering, Zhejiang University, Hangzhou 310027, China
E-mail: flniu@163.com

torque spectrum under stable motor conditions [9].

In order to resolve the above problems, this paper presents a new fault-diagnosis method based on the advantages of HHT in analyzing the non-stationary signal and the continuous variety of the fault feature torque frequency. Experimental results demonstrate that the method can not only detect the rotor fault exactly but also give the number of rotor broken bars according to the magnitude of the intrinsic mode function (IMF), which includes the rotor fault information. This gives us a new way to analyze the severity of the rotor fault.

2 Hilbert-Huang transform

2.1 Definition of instantaneous frequency

For an arbitrary time data, $X(t)$, we can always have its Hilbert transform (HT), $Y(t)$, as

$$Y(t)=\frac{1}{\pi}\int_{-\infty}^{+\infty}\frac{X(\tau)}{t-\tau}\mathrm{d}\tau \tag{1}$$

Its reverse transform is $X(t)=\frac{1}{\pi}\int_{-\infty}^{+\infty}\frac{Y(\tau)}{t-\tau}\mathrm{d}\tau$. With this definition, $X(t)$ and $Y(t)$ form the complex conjugate pair, so we can have an analytic signal, $Z(t)$, as

$$Z(t)=X(t)+\mathrm{j}Y(t)=a(t)\mathrm{e}^{\mathrm{j}\theta(t)} \tag{2}$$

in which

$$a(t)=[X(t)^2+Y(t)^2]^{\frac{1}{2}},\quad \theta(t)=\arctan\frac{Y(t)}{X(t)} \tag{3}$$

Thus, the HT provides a unique way of defining the magnitude and phase of a signal. Essentially, Eq. (1) defines the HT as the convolution of $X(t)$ with $1/t$. It emphasizes the local properties of $X(t)$ and is the best local fit of an amplitude and phase varying trigonometric function to $X(t)$. Based on this, we can define the instantaneous frequency as

$$\omega=\frac{\mathrm{d}\theta(t)}{\mathrm{d}t} \tag{4}$$

2.2 Intrinsic mode function components

Using the local restrictive conditions (that the local mean of the data being zero and the number of extrema and the number of zero crossings must be equal) to take the place of the global restrictive conditions, we can define a meaningful instantaneous frequency defined by the HT.

An intrinsic mode function that satisfies the following two conditions can thus be defined:

1) In the whole data, the number of extrema and the number of zero crossings must be either equal or different at most by one;

2) At any point, the mean value of the envelope defined by the local maxima and the envelope defined by the local minima is zero.

Having defined IMF, we will show that the definition given in Eq. (4) gives the best instantaneous frequency. An IMF after the HT can be expressed as in Eq. (2). If we perform a Fourier transform on $Z(t)$, we have

$$W(\omega)=\int_{-\infty}^{+\infty}a(t)\mathrm{e}^{\mathrm{j}\theta(t)}\mathrm{e}^{-\mathrm{j}\omega t}\mathrm{d}t=\int_{-\infty}^{+\infty}a(t)\mathrm{e}^{\mathrm{j}(\theta(t)-\omega t)}\mathrm{d}t \tag{5}$$

Then by the stationary phase method, the maximum contribution to $W(\omega)$ is given by the frequency satisfying the condition

$$\frac{\mathrm{d}}{\mathrm{d}t}(\theta(t)-\omega t)=0 \tag{6}$$

Therefore, Eq. (4) follows. This is a much better definition for instantaneous frequency than the zero-crossing frequency. Furthermore, it agrees with the definition of frequency for the classic wave theory.

As given in Eq. (6), the frequency defined through the stationary phase condition agrees also with the best fit sinusoidal function locally; therefore, we do not need a whole oscillatory period to define a frequency value. We can define it for every point with the value changing from point-to-point. In this sense, even a monotonic function can be treated as part of an oscillatory function and have instantaneous frequency assigned according to Eq. (4).

But for a complicated signal, we can have more than one instantaneous frequency at a time locally. In order to use this definition of instantaneous frequency, we have to decompose an arbitrary data into IMF components from which an instantaneous frequency value can be assigned to each IMF component.

2.3 The empirical mode decomposition

In order to decompose a complicated non-stationary signal into IMF components, Huang proposed the empirical mode decomposition method [10]. We also call it as local wave decomposition because the method is based on the local character of the signal.

For an arbitrary time data, X(t), We define m_1 as the mean of the two envelopes defined by its local maxima and minima separately, and the difference between the data and m_1 is the first component, h_1, i.e.,

$$X(t)-m_1=h_1 \tag{7}$$

Ideally, h_1 should be an IMF. In reality, however, the envelope mean may be different from the true local mean for complicated non-stationary data, some asymmetric wave forms can still exist. In order to eliminate riding waves and let the wave become more symmetrical, the above process should repeat k times till h_k satisfies the requirements. Then we can get the first IMF component c_1 (h_k is treated as the original data in the following process).

We can separate c_1 from the rest of the data by

$$X(t)-c_1=r_1 \tag{8}$$

The residue, r_1, can be treated as the new data and we

will achieve the following result when we perform the same process for n times:

$$\begin{cases} r_1 - c_2 = r_2 \\ r_2 - c_3 = r_3 \\ \quad \vdots \\ r_{n-1} - c_n = r_n \end{cases} \tag{9}$$

By summing up Eqs.(8)-(9), we finally obtain

$$X(t) = \sum_{i=1}^{n} c_i + r_n \tag{10}$$

Thus, we decompose the original data into n IMF components $c_1, \cdots, c_n$ and a residue r_n, which can be either the mean trend or a constant. The decomposition is completed when the number of local extrema of the final residue r_n is less than two.

2.4 The Hilbert spectrum

After performing HT on each component as described in Eq.(10), we can express the data in the following form:

$$X(t) = \mathrm{Re}\sum_{i=1}^{n} a_i(t)\mathrm{e}^{\mathrm{j}\phi_i(t)} = \mathrm{Re}\sum_{i=1}^{n} a_i(t)\mathrm{e}^{\mathrm{j}\int \omega_i(t)\mathrm{d}t} \tag{11}$$

Here we have left out the residue r_n and Re denotes the real part of a number. Eq.(11) is defined as the Hilbert magnitude spectrum, or Hilbert spectrum for short,

$$H(\omega, t) = \mathrm{Re}\sum_{i=1}^{n} a_i(t)\mathrm{e}^{\mathrm{j}\int \omega_i(t)\mathrm{d}t} \tag{12}$$

We can also define the marginal spectrum as

$$h(\omega) = \int_{-\infty}^{+\infty} H(\omega, t)\mathrm{d}t \tag{13}$$

The above EMD together with the corresponding Hilbert spectrum analysis method are called as HHT. On the one hand, it decomposes a signal into some IMF components with EMD method; on the other hand, it resolves the instantaneous frequency for each IMF component with the Hilbert transform.

In fact, HHT has the advantages of the common signal analysis method. For example, the EMD first achieves the high frequency component, then the low and the lower frequency components of a signal.

The expanding express of Fourier transform (FT) is:

$$X(t) = \mathrm{Re}\sum_{i=1}^{\infty} a_i \mathrm{e}^{\mathrm{j}\omega_i t} \tag{14}$$

in which a_i and ω_i are constant. Therefore, HHT can be considered as the generalized FT.

There are more advantages of the HHT. It defines the IMF for the first time. The magnitude of the IMF is allowed to vary, and the experienced bases are not required when performing the EMD. This is a breakthrough to the traditional idea in which only the constant magnitude periodical oscillations can be used as the base signal. The instantaneous frequency of each IMF component is not only related with sample frequency, but also varying with the signal, so the EMD has the self-adaptive properties. But when the wavelet bases and the scales are selected, the wavelet decomposition is related only with the scales and sample frequency, which does not have the self-adaptive properties. The instantaneous frequency is defined as the differential of the instantaneous phase, thus with no requirement of the whole wave to define the local frequency. The wavelet transform is in fact the adjustable window FT. There will be energy leakages when performing wavelet transform on a signal due to the length-limited wavelet base and thus it is difficult to analyze the time-frequency character exactly. However, the research on HHT only started in 1998. The potential merits need to be explored and the associated analysis methods need to be perfected in the future.

3 Computation of the electromagnetic torque

3.1 Computation model of the electromagnetic torque

In $\alpha, \beta, 0$ reference frame, the electromagnetic torque equation can be expressed as

$$T_{\mathrm{em}} = p(\varphi_\alpha i_\beta - \varphi_\beta i_\alpha) \tag{15}$$

in which $\varphi = \int (V - iR)\mathrm{d}t$, p is pole pairs and R is the stator resistance. Using the motor terminal data, it can be rewritten as

$$T_{\mathrm{em}} = \frac{p\sqrt{3}}{6}\{(2i_A + i_C) \times \int [V_{CA} - R(i_C - i_A)]\mathrm{d}t - (i_C - i_A) \times \int [-V_{BA} - R(i_C + 2i_A)]\mathrm{d}t\} \tag{16}$$

Therefore, this method is noninvasive because the electromagnetic torque can be calculated from the terminal voltages and currents. Ref.[11] pointed out that the electromagnetic torque for a faulty motor can be achieved from the symmetrical healthy motor model.

3.2 Data acquisition and computation results of the electromagnetic torque

A small induction motor is used for experimental validation. A set of additional cage rotors fabricated with the following faults, one rotor broken-bar, two adjacent rotor broken-bars, are used for the test. The motor operates under no load conditions. Its nominal data are: P_N=370 W, U_N=380 V, I_N = 0.7 A, n_N = 1 400 r/min, and the supply frequency is 50 Hz.

In order to get accurate torque, the four channels should sample signal synchronously because the electromagnetic torque comprises the phase information between the voltages and currents. The sample rate is 40 kHz (10 kHz for each channel) and software synchronization is adopted in this paper. The skin effect and temperature variation are left out, that is, the stator resistance is considered as constant during the startup of the test motor.

Figures 1-3 show the electromagnetic torque wave-forms when the motor starts normally, with one and two adjacent rotor broken-bars respectively.

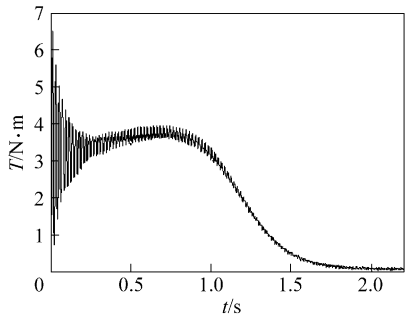

Fig. 1 Electromagnetic torque of the healthy motor

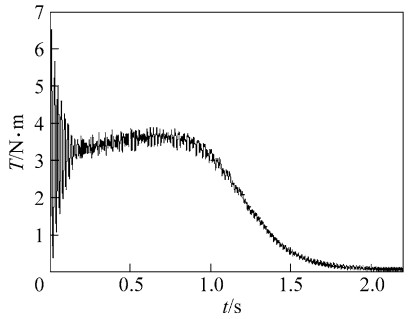

Fig. 2 Electromagnetic torque of the one rotor broken-bar motor

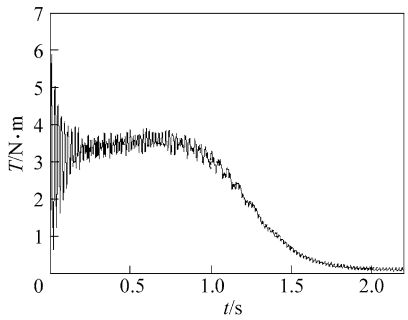

Fig. 3 Electromagnetic torque of the two adjacent rotor broken-bars motor

Figure 1 shows that the electromagnetic torque only contains transient fundamental component at the startup, and will be a DC component when the motor reaches the stable condition. The stable torque is near zero because the test motor is with no load. Fig. 2-3 indicate it will contain corresponding fault feature component for the rotor broken-bar motors. The fault feature component is more significant after complete attenuation of the fundamental component. Its magnitude for the two adjacent rotor broken-bars motor is larger than that for the one rotor broken-bar motor. According to the following analysis, rotor broken-bar fault can be easily detected by performing HHT on the fault feature component.

4 Rotor fault diagnosis based on HHT

4.1 EMD of the startup electromagnetic torque

From principles of EMD, we know that construction of the envelope line, which influences the whole decomposition process and results, is the key to HHT. The upper and lower envelopes determined by local maxima and minima are used to achieve the local mean. Once the extrema are identified, all the local maxima are connected by a cubic spline line as the upper envelope. Repeat the procedure for the local minima to produce the lower envelope. The upper and lower envelopes should cover all the data between them. Their mean is defined as the mean of the whole data and we can perform EMD on the data using them.

Meanwhile, the following processes are performed before decomposition in order to detect rotor fault feature component fast and accurately:

1) The electromagnetic torque in the interval from the transient fundamental component complete attenuation to the stable condition (0.8 s< t <1.3 s) is adapted in order to get rid of the influences of the transient fundamental component.

2) Since the frequency variation range of the fault feature component is 100 Hz $\rightarrow f \rightarrow$ 0 Hz during the whole startup process, we can use a low pass filter, whose cutoff frequency is 100 Hz, to eliminate the high frequency interferences derived from experimental error.

Figures 4-6 give us the IMF waveforms after EMD of startup electromagnetic torque for the healthy as well as one and two adjacent rotor broken-bars motor. From upper to lower, they correspond to $c1$, $c2$ and the residue component r respectively.

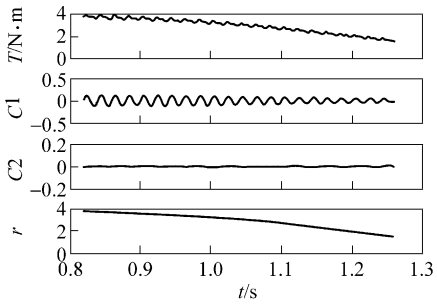

Fig. 4 EMD of startup electromagnetic torque of the healthy motor

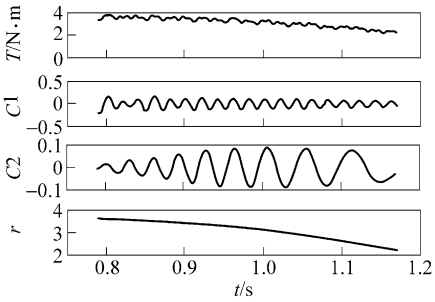

Fig. 5 EMD of startup electromagnetic torque of the one rotor broken bar motor

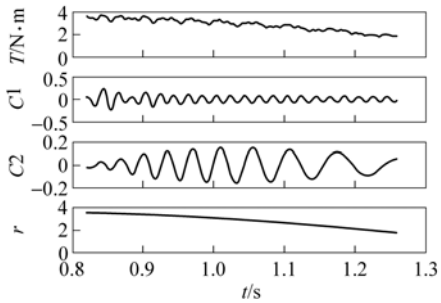

Fig. 6 EMD of startup electromagnetic torque of the two adjacent rotor broken-bars motor

As we all know, the electromagnetic torque only comprises the transient fundamental component and a variant trend component. Therefore, ideally, the electromagnetic torque does not need decomposition because in the adapted interval the transient fundamental component is attenuated completely. The variant trend component is just the so-called residue component. But in reality, the filtered startup electromagnetic torque still comprises feeble fundamental component, $c1$, which is introduced by experimental error and its magnitude should be equal for the different fault conditions. According to the above analysis, the electromagnetic torque in the interval adapted should comprise three components, that is, two IMF components and a residue component. Consequently, after two rounds of EMD, every IMF can be achieved, and that, $c1$ denotes the feeble fundamental component derived from experimental error, $c2$ denotes the IMF component including fault information and r denotes the variant trend component respectively. The cubic spline interpolation is used to obtain the envelopes in this paper. At the two ends there will be swing, which will introduce errors because they perhaps are not extrema of the data. However, it seems not to matter for extraction of rotor broken-bar fault feature frequency.

4.2 Rotor fault feature frequency extraction results and their analysis

Figure 4 shows that the magnitude of $c2$ is almost zero, which implies that the motor has no fault. So, for the healthy motor, the electromagnetic torque just contains the experimental error component, $c1$, and the variant trend component, r. But Figs. 5-6 show that besides the experimental error component $c1$, and the variant trend component r, the electromagnetic torque also contains $c2$, which includes fault information for those rotor broken-bar motors. The instantaneous frequency variation law of $c2$ can be calculated based on HHT, as shown in Figs. 7-8 respectively.

From Figs. 7-8, we find that the frequency of $c2$ varies continuously. Furthermore, its variation is consistent with the variation law of the fault feature component. Thus, the rotor broken-bar fault can be easily detected. The startup process-based method can overcome the confusion derived from the fluctuation of the supply frequency or the load fluctuation because their frequency variation laws are impossibly similar with the fault feature component. Moreover, the amplitude of $c2$ in Fig. 6 is approximately two times of that in Fig. 5, which agrees with the ratio of rotor broken-bar number. It demonstrates the feasibility of this method for decomposition of the fault feature component. Also, the magnitude of the rotor fault feature component, which also reflects its energy size, gives us a quantitative numerical criterion for evaluating the rotor fault severity of the induction motor.

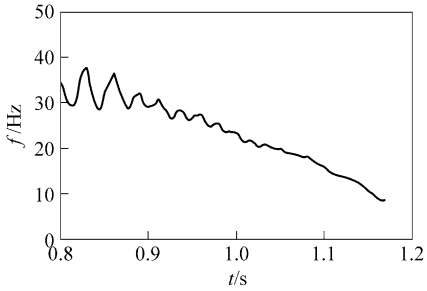

Fig. 7 Instantaneous frequency of IMF component $c2$ of the one rotor broken bar motor

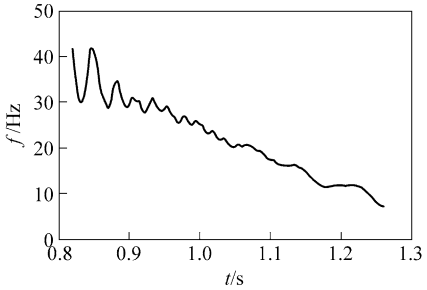

Fig. 8 Instantaneous frequency of IMF component $c2$ of the two adjacent rotor broken bars motor

5 Conclusions

This paper presents a new method for rotor broken-bar fault diagnosis of induction motors based on the startup electromagnetic torque signal. As the electromagnetic torque represents the combined effect of all the flux linkages and currents in both stator and rotor, it is highly sensitive to any asymmetrical operating condition. Theoretically, next to rotor current, the electromagnetic torque is the diagnostic medium most affected by rotor faults. According to the non-stationary property of the startup electromagnetic torque, it can be decomposed into several IMF components with EMD of HHT. Then, using the instantaneous frequency extraction principle of the HT, the rotor broken-bar fault characteristic frequency can be exactly extracted from the IMF component, which includes the rotor fault information. Experimental results

demonstrate that this method can overcome the confusion derived from the fluctuation of the supply frequency or the load to detect the rotor broken-bar fault exactly. Moreover, the magnitude of the IMF, which includes the rotor fault information, can also give the number of rotor broken bars. Therefore this method gives us a new way to evaluate the rotor fault severity.

References

1. Ethan, Y. H., Song, Condition monitoring techniques for electrical equipment-A literature survey, IEEE Trans. Power Deliv., 2003, 18(1): 4–13
2. Belling A., On-field experience with online diagnosis of large induction motors cage failures using MCSA, IEEE Trans. Ind. Appl., 2002, 38(4), 1045–1053
3. Belling A., Foreknow Flippest, et al., Quantitave evaluation of induction motor broken bars by means of electrical signature analysis, IEEE Trans. Ind. Appl., 2001, 37(5), 1248–1255
4. Liu Z., Yin X., et al., On-line monitoring and diagnosis way based on spectrum analysis of Hilbert modulus in induction motors, Procedings of the CSEE, 2003, 23(7):158–161
5. Hou X., Wu G., et al., A method for detecting rotor faults in asynchronous motors based on the square of the park's vector modulus, Procedings of the CSEE, 2003, 23(9): 137–140
6. Cruz S. M. A., Marques Cardoso A. J., Rotor cage fault diagnosis in three-phase induction motors by the total instantaneous power spectral analysis, Industry Applications Conference, 1999. Thirty-Fourth IAS Annual Meeting, 3: 1929–1934
7. Trzynadlowski A. M., Ewen Ritchie, Comparative investigation of diagnostic media for induction motors: A Case of Rotor Cage Faults, IEEE Trans. Ind. Electron., 2000, 47(5), 1092–1099
8. Hsu J. S., Monitoring of defects in induction motors through air-gap torque observation, IEEE Trans. Ind. Appl., 1995, 31(5): 1016–1021
9. Zhang Z., Ren Z., et al., A novel method of motor faulted rotor detection based on wavelet ridge, Procedings of the CSEE, 2003, 23(1): 97–101
10. Huang N. E., The empirical mode decomposition and the hilbert spectrum for nonlinear and non-stationary time data analysis, Proc. R. Soc. Lond. A., 1998, 454: 903–995
11. Thomas V. V., Vasudevan K., et al., Online cage rotor fault detection using air-gap torque spectrum, IEEE Trans. Energy Convers., 2003, 18(2): 265–270